Available online at www.sciencedirect.com
ScienceDirect
Journal of the European Ceramic Society 31 (2011) 1293–1303
www.elsevier.com/locate/jeurceramsoc

Phase diagrams of the systems Al_2O_3–ZrO_2–$Ln(Y)_2O_3$ as a source of multiphase eutectics for creating composite structural and functional materials

S. Lakiza *, L. Lopato

Frantsevich Institute for Problems of Materials Science, Krzizanovsky 3, 03142 Kyiv, Ukraine

Available online 15 January 2011

Abstract

Phase equilibria in the ternary systems Al_2O_3–ZrO_2–Ln_2O_3 (Ln = La, Nd, Sm, Gd, Er, Yb and Y) were investigated by identical methods in all range of concentrations and 1250–2700 °C temperature range using differential and derivative in solar furnace thermal analysis in controlled medias, X-ray diffraction phase analysis, local X-ray spectral analysis, chemical analysis, electron and optical microscopy, petrography. The phase diagrams of the systems studied are presented as isothermal at 1650 °C sections and melting diagrams. The interaction in the systems is characterized by the absence of ternary compounds and regions of appreciable solid solutions based on the binary compounds and components. Only narrow regions of ternary solid solutions were discovered at high temperatures by CALPHAD method and because of existing small solubility on the base of ZrO_2 in the binary bounding system Al_2O_3–ZrO_2. The phase equilibria in the systems are determined by zirconia as the most stable compound. Solidification in the systems is completed in eutectic reactions. The established interaction regularities allowed to forecast interaction and phase diagrams construction in systems with other lanthanides (Ce, Pr, Pm, Eu, Tb, Dy, Ho, Tm, Lu). New 13 quasibinary and 26 ternary eutectics were found for the first time. Their temperatures rise from 1660 °C for the La_2O_3 system to 1840 °C for the Lu_2O_3 system. Fluorite-type phases equilibrate with garnet-type phases for the systems from Tb_2O_3 to Lu_2O_3. In the systems from Pr_2O_3 to Gd_2O_3 they equilibrate with perovskite-type phases and β-Al_2O_3. On the base of microstructure investigations it was established that three-phase alumina-rich eutectics crystallizes according to the mechanism of cooperative growth. It opens up possibilities to obtain composite materials using directional solidification method.
© 2010 Elsevier Ltd. All rights reserved.

Keywords: Alumina; Zirconia; Lanthanides oxides; Yttria; Phase diagrams

1. Introduction

The systems Al_2O_3–ZrO_2–$Ln(Y)_2O_3$ plays a vital part in material science of modern ceramics. Wide scale of materials for solid oxide fuel cells (SOFC), thermal barrier coatings (TBC), high-temperature structural and functional materials can be constructed in these systems. Special attention during last decade has been paid to the development of heat-resistant materials with high strength and phase stability at temperatures above 1600 °C. Up to this time there are no structural materials except directionally solidified oxide eutectics (DSE), which could be used in oxidizing environment and retain enough strength at such high temperatures.

Development of new multiphase materials, especially composites, as the first step needs constructing phase diagrams of the systems in which desired materials are planned to obtain. This is why phase diagrams of the Al_2O_3–ZrO_2–$Ln(Y)_2O_3$ (Ln = lanthanides) are of a great significance.

Phase diagrams construction of the systems Al_2O_3–ZrO_2–$Ln(Y)_2O_3$ was based on the basis of much efforts on constructing binary phase diagrams, performed in the previous decades by a number of scientists. Among them it is necessary to refer to the works of Rouanet,[1] Bondar,[2] Mizuno,[3] Wu,[4] and many others.[5–16]

Information on Al_2O_3–ZrO_2–$Ln(Y)_2O_3$ phase diagrams was very poor. Only isothermal sections at undersolidus temperatures were known for the system Al_2O_3–ZrO_2–Y_2O_3.[17,18]

2. Experimental details

Specimens were obtained by both chemical method and by melting the component oxides. Powders of $Al(NO_3)_3{\cdot}9H_2O$, $ZrO(NO_3)_2{\cdot}2H_2O$ with purity 99.9% (Donetskij zavod khimreaktiviv, Donetsk) and Ln_2O_3/Y_2O_3 (99.99%) were used for

* Corresponding author.
E-mail address: sergij_lakiza@ukr.net (S. Lakiza).

0955-2219/$ – see front matter © 2010 Elsevier Ltd. All rights reserved.
doi:10.1016/j.jeurceramsoc.2010.12.004

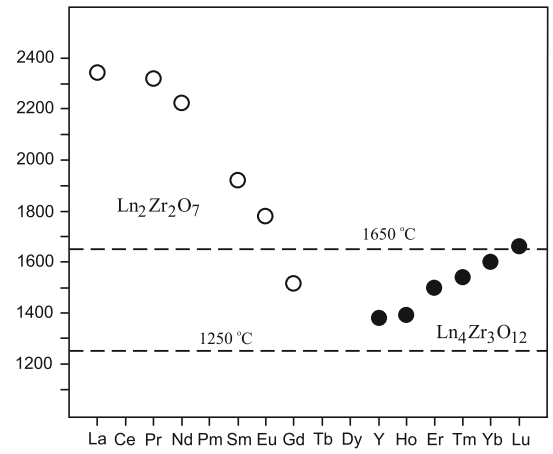

Fig. 1. The upper temperature stability limits for superstructures $Ln_2Zr_2O_7$ and $Ln_4Zr_3O_{12}$ *vs* lanthanides atomic number.[21]

chemical route preparations. Both salts and Ln_2O_3/Y_2O_3 were dissolved in water with some droplets of concentrated nitric acid added, dried, calcined at 900 °C in air and pressed into pellets 5 mm in diameter and 5 mm in height. Powders of alumina (99.9%), zirconia (99.95%), Ln_2O_3/Y_2O_3 (99.99%) from Donetskij zavod khimreaktiviv, Donetsk, were used as raw materials. The appropriate quantities of oxides were blended in an agate mortar with ethanol, dried and pressed into pellets of the same dimensions.

For the constructing of isothermal sections chemically derived samples were annealed at 1250 and 1650 °C for the time necessary to attain equilibrium, established by unchanging XRD patterns. Other samples were fired at 1250 °C in air for 6 h, then melted in molybdenum pots in a DTA device[19] at total pressure of H_2 about 1.2 atm and annealed below the solidus temperature for 1 h. The specimens were investigated by DTA in H_2 at temperatures up to 2300 °C,[19] derivative thermal analysis in solar furnace up to 2800 °C,[20] X-ray (DRON-1.5, Burevestnik, St.-Petersburg), petrographic (MIN-8 optical microscope,

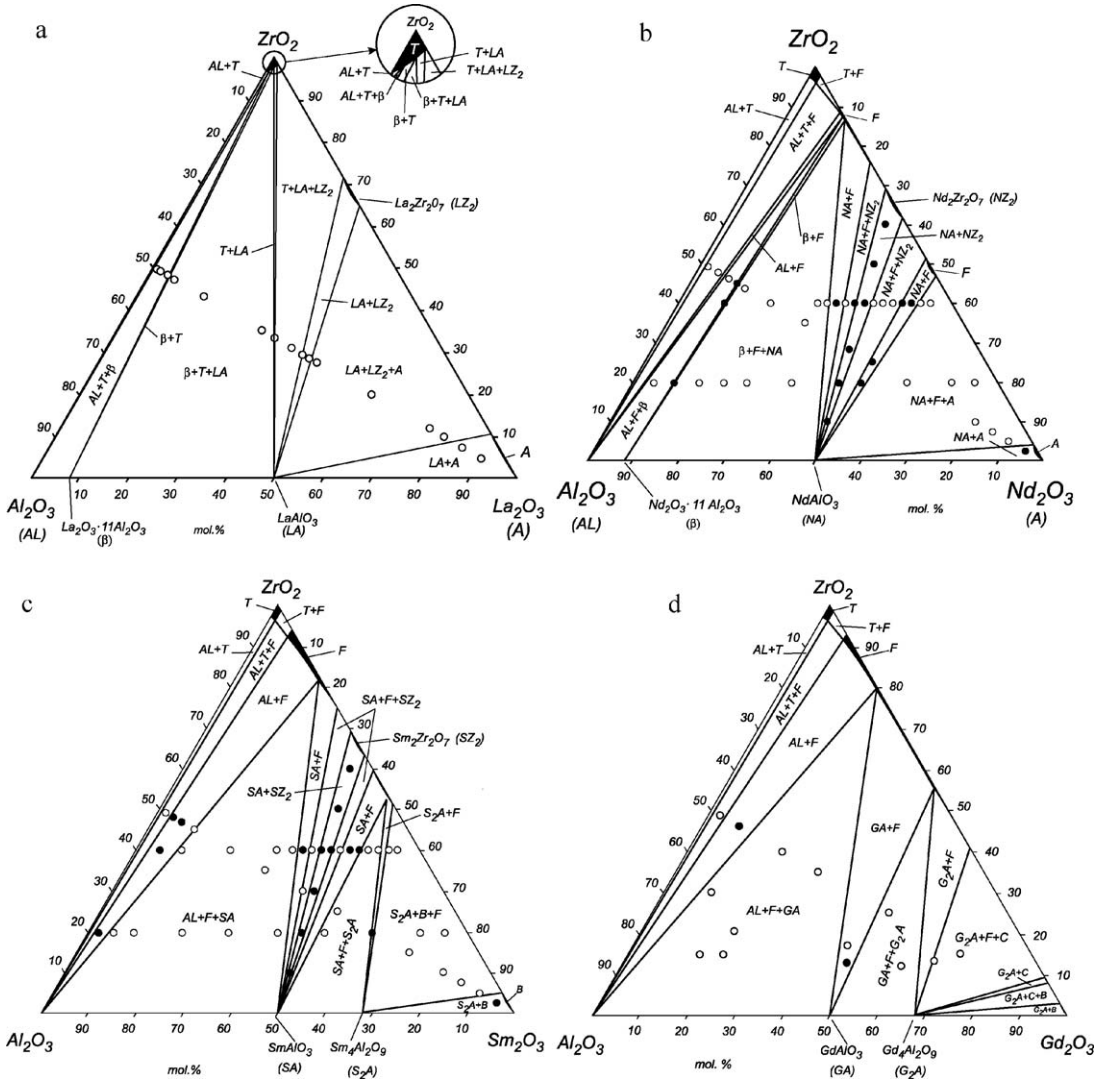

Fig. 2. Isothermal sections at 1650 °C of some Al_2O_3–ZrO_2–$Ln(Y)_2O_3$ phase diagrams: (A) a – La_2O_3; b – Nd_2O_3; c – Sm_2O_3; d – Gd_2O_3; (B) a – Y_2O_3; b – Er_2O_3; c – Yb_2O_3.

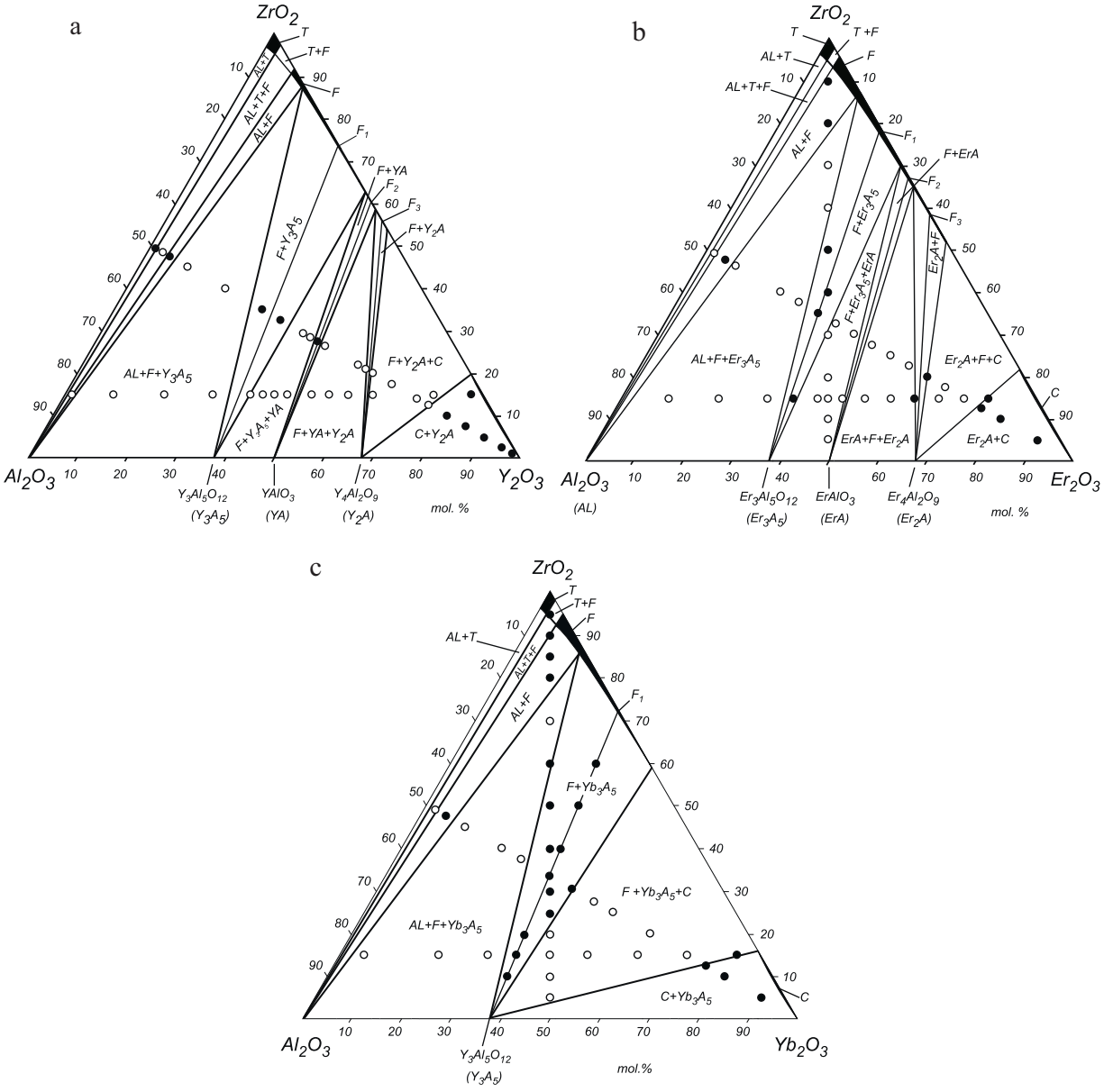

Fig. 2. (*Continued*).

LOMO, St.-Petersburg) and microstructure phase (JEOL JSM-6490LV) analysis. The accuracy for XRD measurement came to ±0.0003 nm, for refractive indexes measured with immerse liquids ±0.003, with alloys – ±0.02.

3. Results and discussion

After analysis of interaction in the binary bounding systems Al_2O_3–ZrO_2, Al_2O_3–Ln(Y)$_2O_3$ and ZrO_2–Ln(Y)$_2O_3$ it became clear that the construction of the Al_2O_3–ZrO_2–Ln(Y)$_2O_3$ phase diagrams depends on interaction in the systems Al_2O_3–Ln(Y)$_2O_3$. The number of binary aluminates in these systems determines the construction of the ternary phase diagrams. So seven systems with La, Nd, Sm, Gd, Er and Yb oxides as well as Y_2O_3 were selected for complete phase diagrams construction in the temperature range 1250–2700 °C. Such investigation is very important as far as it was performed under the same methods of sample preparation and analysis.

Temperatures for isothermal sections of phase diagrams at 1250 and 1650 °C were taken after analyzing the temperature stability limits of superstructure compounds in the systems ZrO_2–Ln_2O_3.[21] These limits versus Ln(Y) atomic numbers are presented in Fig. 1.

In this article we accepted the following shorthand notations of phases presented in the phase diagrams: T, F – ZrO_2-based solid solutions with tetragonal (space group $P4_2/nmc$) and cubic fluorite ($Fm3m$) structures, accordingly; A, B, C, H, X – Ln_2O_3-based solid solutions with low-temperature hexagonal ($P\bar{3}m1$), monoclinic ($C2/m$), low-temperature cubic ($Ia3$), high-temperature hexagonal ($P6_3/mmc$) and high-temperature cubic ($Im3m$) structures, accordingly; AL – Al_2O_3 ($Fd\bar{3}ma$), β – $Ln_2O_3{\cdot}11Al_2O_3$ with hexagonal ($P6_3/mcm$) structure, LnA

– $LnAlO_3$ with perovskite-like (*Pbnm*) structure, Ln_3A_5 – $Ln_3Al_5O_{12}$ with garnet-like (*Ia*3*d*) structure, Ln_2A – $Ln_4Al_2O_9$ with monoclinic ($P2_1/c$) structure, LnZ_2 – $Ln_2Zr_2O_7$ with pyrochlore-like (*Fd*3*m*) structure.

In Fig. 2 isothermal sections at 1650 °C and in Fig. 3 – melting diagrams of the systems studied are presented.[5,22–29] The main features of interaction in these systems are the lack of quasiternary compounds and appreciable regions of solid solutions based on quasibinary compounds and components. The most thermodynamically stable phases are oxides-components. Zirconia, as the most refractory phase, determines interaction in the systems. This phase equilibrates with the majority of other phases of the systems. Its primary crystallization fields gradually increases from La to Yb. Phase transformations of $^{F\leftrightarrows T}$ ZrO_2-based solid solutions and $^{X\leftrightarrows H\leftrightarrows A\leftrightarrows B\leftrightarrows C}$ of Ln_2O_3-based solid solutions realize as liquid involving transformation processes. Thermal stability of compounds-superstructures with the pyrochlore-type structure $Ln_2Zr_2O_7$ and with rhombohedral structure $Zr_3Ln_4O_{12}$ formed in the binaries ZrO_2–Ln_2O_3 does not change with adding third component (Al_2O_3) that is represented in the isothermal sections of the phase diagram. Solidification in the systems finishes in eutectic equilibria in the areas close to the binary bounding systems Al_2O_3–$Ln(Y)_2O_3$. The coordinates of firstly found three-phase eutectics from the systems Al_2O_3–ZrO_2–$Ln(Y)_2O_3$ are shown in Table 1.

In Fig. 4 some microstructures of alumina-rich three-phase eutectics in the systems Al_2O_3–ZrO_2–$Ln(Y)_2O_3$ are presented. Microstructure analysis revealed that alumina-rich three-phase eutectics demonstrate cooperative eutectic growth, so they can be obtained as three-phase "in situ" composite by directional solidification. The obtained results revealed that alumina-rich

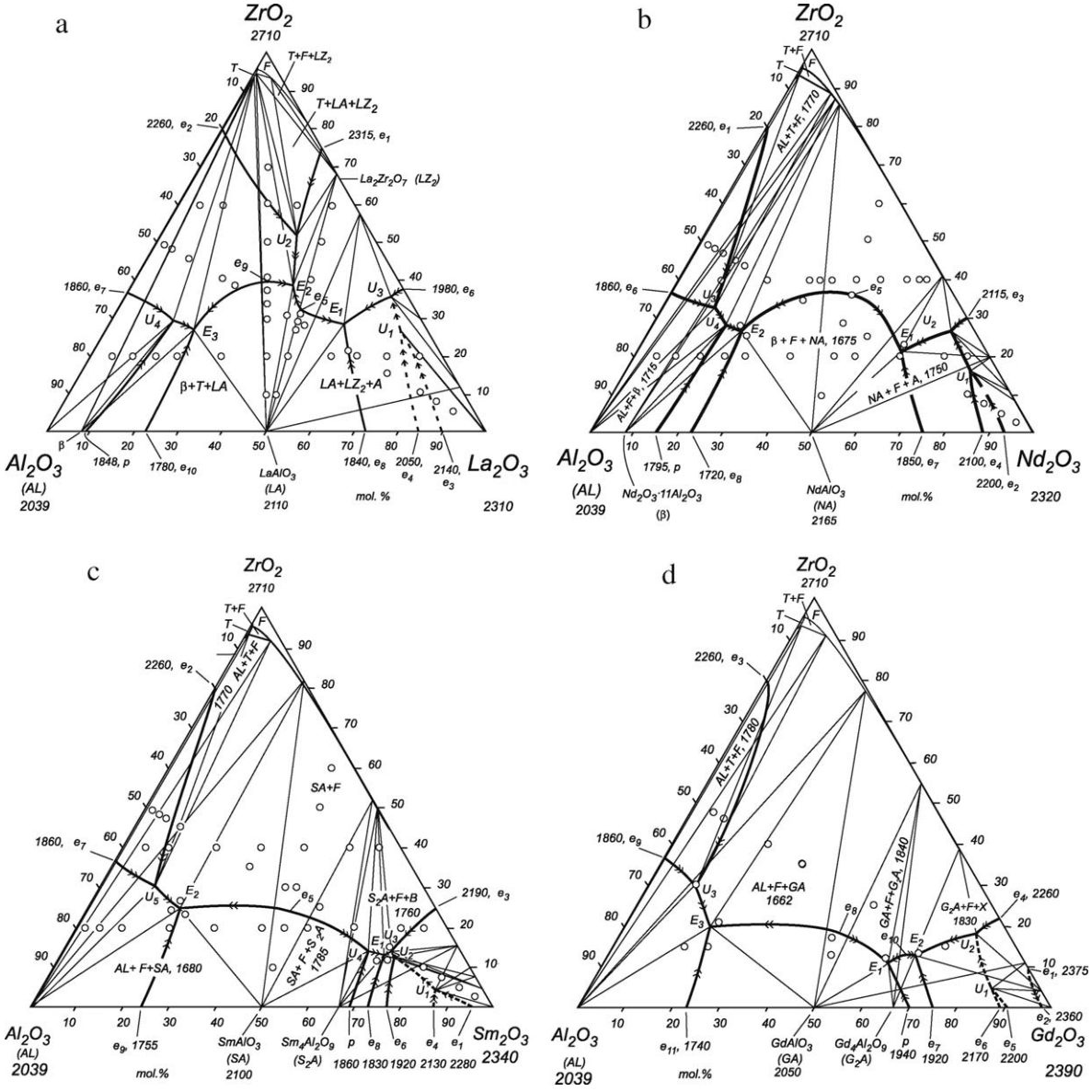

Fig. 3. Melting diagrams of the systems Al_2O_3–ZrO_2–$Ln(Y)_2O_3$: (A) a – La_2O_3; b – Nd_2O_3; c – Sm_2O_3; d – Gd_2O_3; (B) a – Y_2O_3; b – Y_2O_3 (metastable); c – Er_2O_3; d – Yb_2O_3.

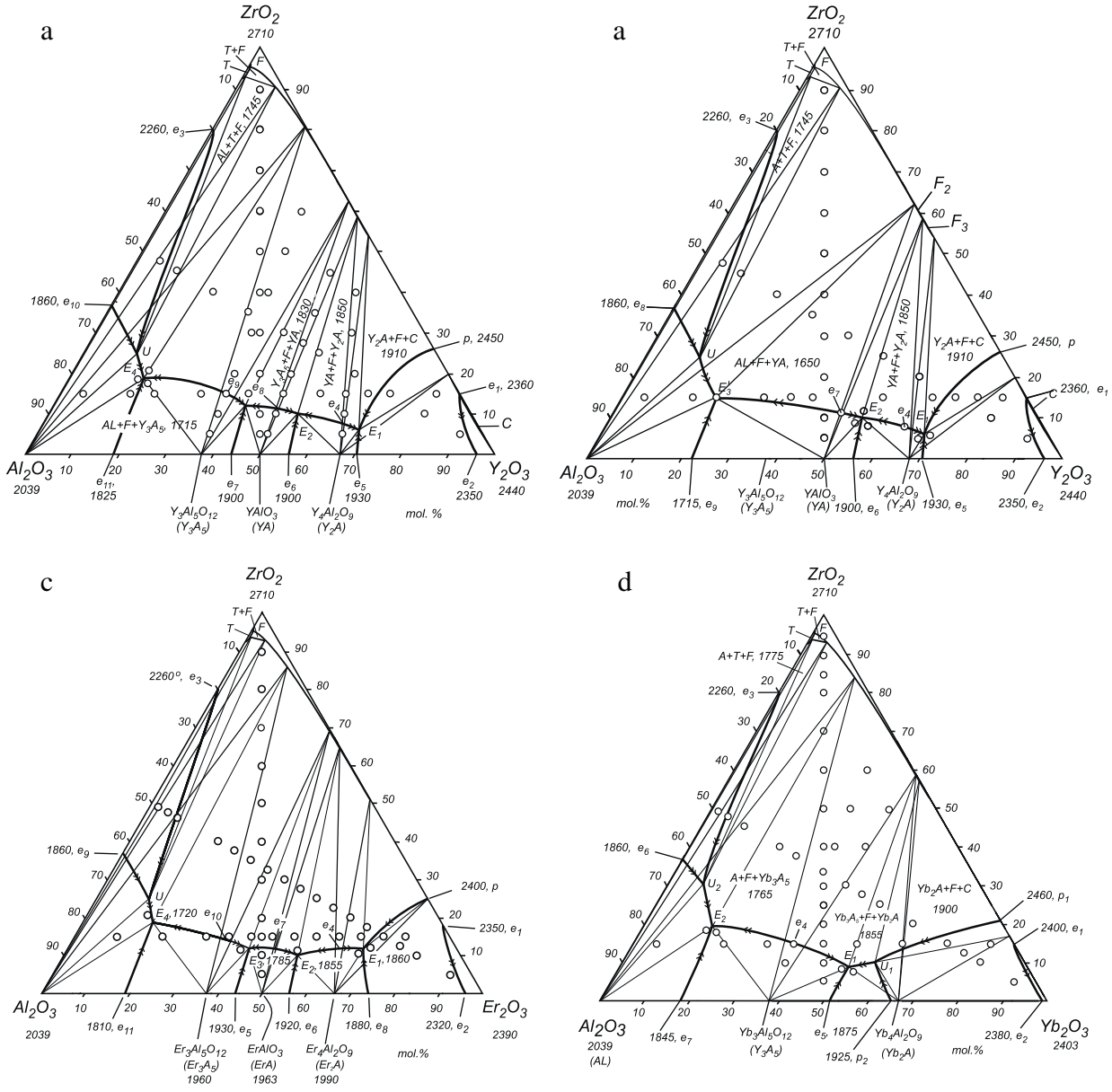

Fig. 3. (*Continued*).

ternary eutectics have similar gross composition, but consist of different set of phases. In these systems according to the lanthanide involved one can get three sets of three-phase eutectics: $Al_2O_3/Ln_3Al_5O_{12}/ZrO_2$, $Al_2O_3/LnAlO_3/ZrO_2$ and β-$Al_2O_3/LnAlO_3/ZrO_2$. This fact increases number of objects for directional solidification and allows choosing material with desirable set of properties for every specific utilization. As it was shown,[30–32] such monocolony eutectic structures are the best high-temperature structural materials and can be used at temperatures up to 1650 °C. They are also proposed as good thermoemitters to convert heat energy into electric power.[33]

The established interaction regularities in the systems Al_2O_3–ZrO_2–$Ln(Y)_2O_3$ (Ln = La, Nd, Sm, Gd, Er, Yb) allowed to forecast interaction and phase diagrams construction in systems with other lanthanides (Ce, Pr, Pm, Eu, Tb, Dy, Ho, Tm, Lu) that were not studied. In Fig. 5 experimental and predicted results on liquidus projections for the systems Al_2O_3–ZrO_2–$Ln(Y)_2O_3$ are presented. The obtained results can be used as a guide for investigating the rest of the Al_2O_3–ZrO_2–$Ln(Y)_2O_3$ phase diagrams. According to this the limited experiments were conducted to verify the coordinates of alumina-rich ternary eutectics predicted. In Table 2 one can find the experimental and predicted coordinates of these ternary eutectics. In Fig. 6 microstructures of some alumina-rich eutectics from unstudied systems Al_2O_3–ZrO_2–$Ln(Y)_2O_3$ are given.

It is interesting to analyze the influence of lanthanide atomic number on interaction in the Al_2O_3–ZrO_2–$Ln(Y)_2O_3$ systems. To answer this question the dependence of alumina-rich eutectics melting temperatures *vs* lanthanide atomic number was compared to the melting temperatures of lanthanide ele-

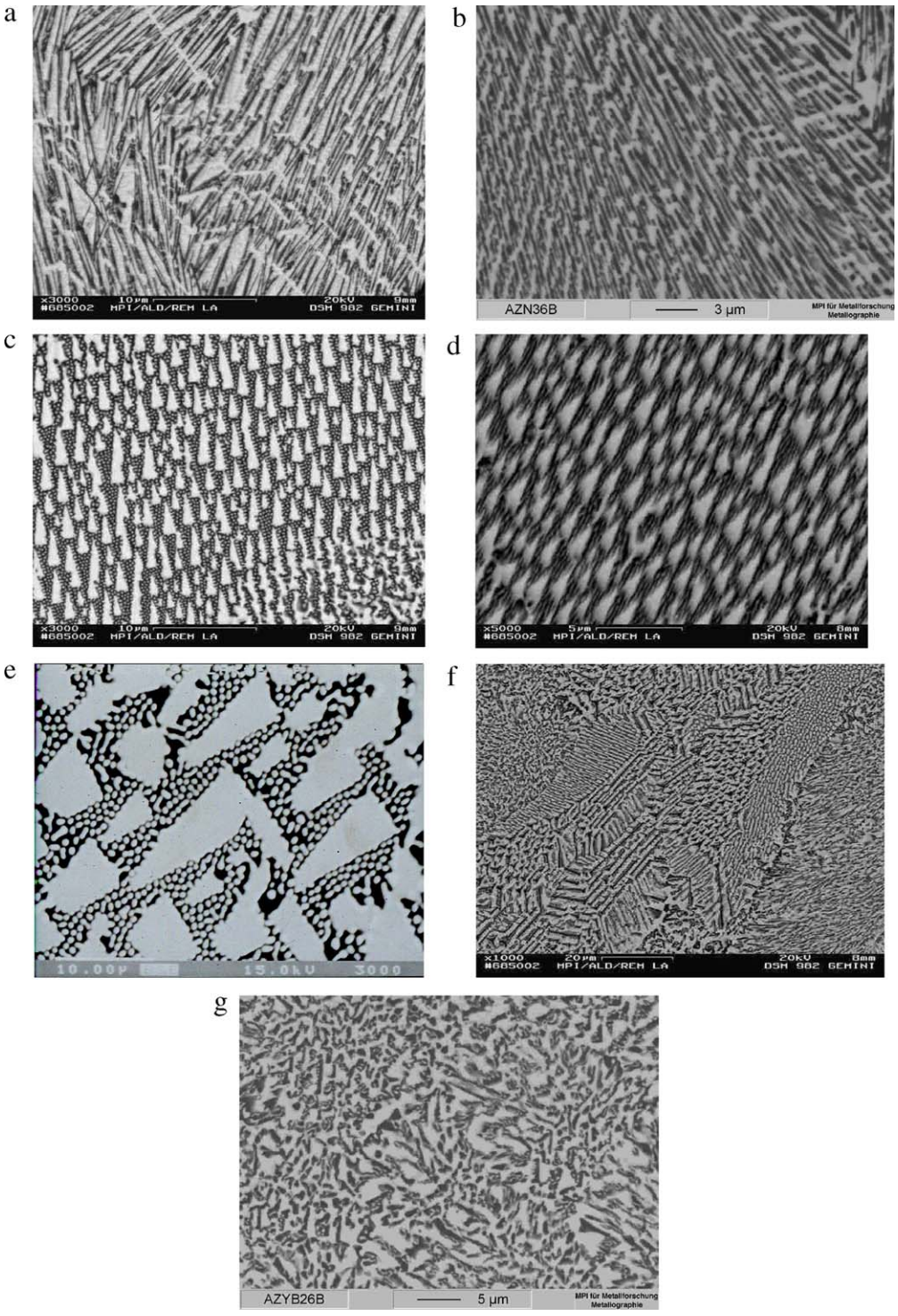

Fig. 4. Microstructures of some alumina-rich three-phase eutectics in the systems Al_2O_3–ZrO_2–$Ln(Y)_2O_3$: a – β-Al_2O_3 + T + $LaAlO_3$, 2000×; b – β-Al_2O_3 + F + $NdAlO_3$, 8000×; c – Al_2O_3 + F + $SmAlO_3$, 3000×; d – Al_2O_3 + F + $GdAlO_3$, 3000×; e – Al_2O_3 + F + $Y_3Al_5O_{12}$, 3000×; f – Al_2O_3 + F + $Er_3Al_5O_{12}$, 1000×; g – Al_2O_3 + F + $Yb_3Al_5O_{12}$, 5000×.

ments, their oxides and lanthanide aluminates (Fig. 7). When comparing these dependences one can make the following conclusions.

Metal lanthanides, their oxides, aluminates as well as three-phase eutectics demonstrate melting temperatures monotony leaps for Ce, Eu, Tm–Yb, that correspond to the free, semiocupied and completely occupied electron configurations of f lanthanides shells.[35] Because for lack of quasiternary compounds and wide areas of ternary solid solutions in the systems studied the influence of electron configurations on interaction in the systems remains when their componency increases, but diminishes.

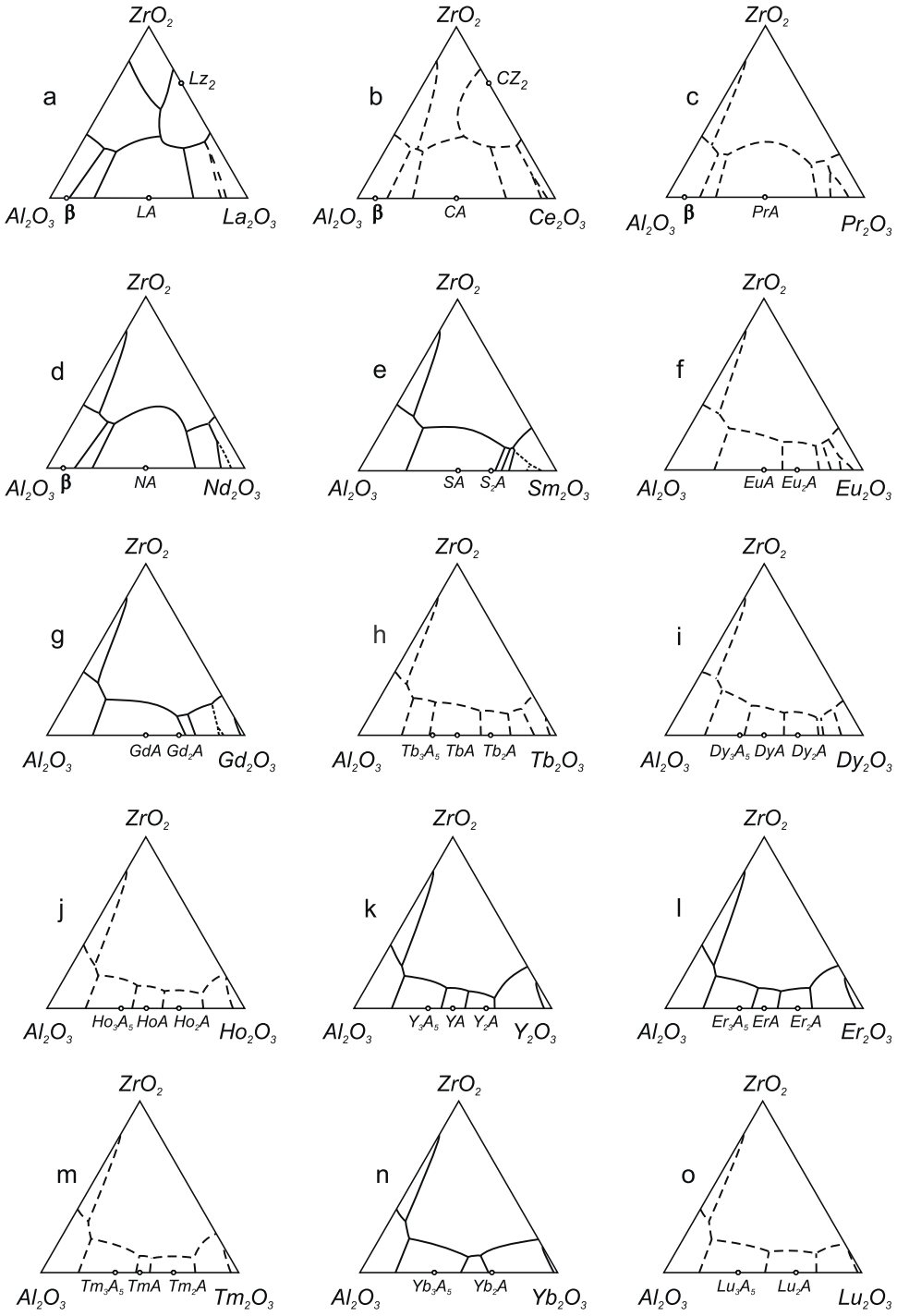

Fig. 5. Experimental and predicted liquidus surface projections of the Al_2O_3–ZrO_2–$Ln(Y)_2O_3$ phase diagrams: systems with: a – La_2O_3; b – Ce_2O_3; c – Pr_2O_3; d – Nd_2O_3; e – Sm_2O_3; f – Eu_2O_3; g – Gd_2O_3; h – Tb_2O_3; i – Dy_2O_3; j – Ho_2O_3; k – Y_2O_3; l – Er_2O_3; m – Tm_2O_3; n – Yb_2O_3; o – Lu_2O_3.

In Fig. 8 the dependences of ZrO_2–Ln_2O_3[1,36] and HfO_2–Ln_2O_3[37–40] binary eutectics melting temperatures *vs* lanthanides atomic number are shown. When comparing them with the same dependences for lanthanides aluminates (Fig. 7) one can conclude that the influence of f lanthanides shell electron configuration is pronounced in the systems Al_2O_3–Ln_2O_3, ZrO_2–Ln_2O_3 and HfO_2–Ln_2O_3. In other words, influence of f lanthanides shell electron configuration on the interaction is restricted on the level of binary systems.

Taking into consideration the literature and experimental data on applications of materials, constructed in binary bounding and ternary Al_2O_3–ZrO_2–$Ln(Y)_2O_3$ systems, in Fig. 9 areas of perspective single phase, two- and three-phase composite, two- and three-phase eutectic materials for application as TBC, SOFC, high-temperature structural materials

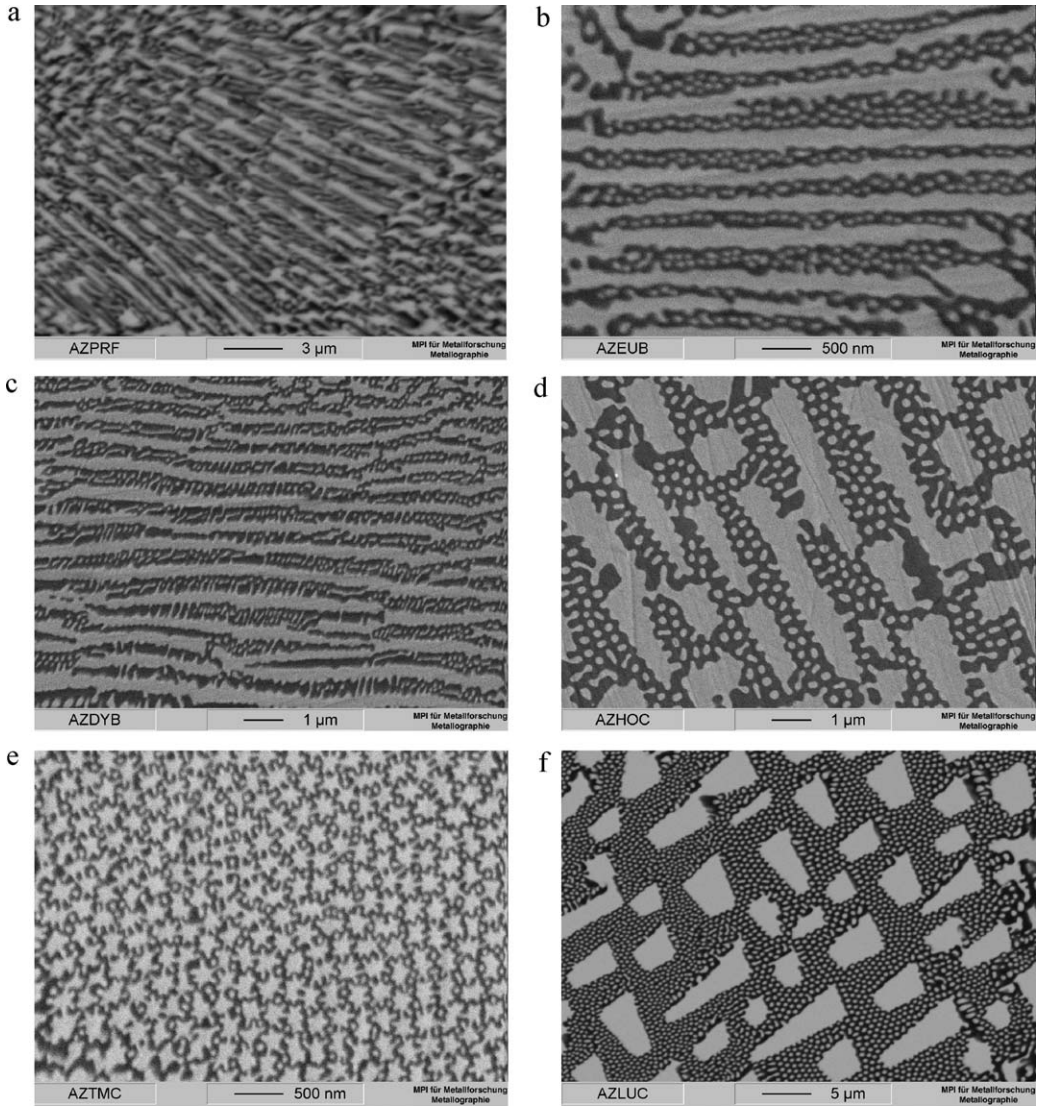

Fig. 6. Microstructures of some Al_2O_3-rich three-phase eutectics in the Al_2O_3–ZrO_2–Ln_2O_3 systems: a – β-Al_2O_3 + T-ZrO_2 + $PrAlO_3$; b – Al_2O_3 + F-ZrO_2 + $EuAlO_3$; c – Al_2O_3 + F-ZrO_2 + $Dy_3Al_5O_{12}$; d – Al_2O_3 + F-ZrO_2 + $Ho_3Al_5O_{12}$; e – Al_2O_3 + F-ZrO_2 + $Tm_3Al_5O_{12}$; f – Al_2O_3 + F-ZrO_2 + $Lu_3Al_5O_{12}$.

Table 1
The coordinates of three-phase eutectics from the Al_2O_3–ZrO_2–Ln_2O_3 systems.

Lanthanide, Y	Eutectic phase compositions	Composition, mol.%			$T_{m.}$, °C
		Al_2O_3	ZrO_2	Ln_2O_3	
La	$LZ_2 + LA + La_2O_3$	18	29	53	1750
	$LZ_2 + T + LA$	26	36	38	1715
	β + T + LA	53	27	20	1665
Nd	β + F + NA	53	26	21	1675
	$NA + F + Nd_2O_3$	19	21	60	1750
Sm	AL + F + SA	55	25	20	1680
	SA + F + B	17	13	70	1760
Gd	AL + F + GA	60	21	19	1662
	$G_2A + F + B$	22	13	65	1830*
	$GA + F + G_2A$	29	11	60	1840*
Y	$AL + F + Y_3A_5$	65	19	16	1715
	$Y_3A_5 + F + YA$	47	12	41	1830
	$YA + F + Y_2A$	37	10	53	1850
	$Y_2A + F + C$	26	6	68	1910
Er	$AL + F + Er_3A_5$	65	19	16	1720
	$Er_3A_5 + F + ErA$	47	12	41	1785
	$ErA + F + Er_2A$	37	10	53	1855
	$Er_2A + F + C$	21	12	67	1860
Yb	$AL + F + Yb_3A_5$	65	20	15	1765
	$Yb_3A_5 + F + Yb_2A$	41	9	50	1885

* Calculated with CALPHAD method.

Table 2
Experimental and predicted melting temperatures, chemical and phase compositions of alumina-rich three-phase eutectics in the Al_2O_3–ZrO_2–$Ln(Y)_2O_3$ systems.

No.	Lanthanide, Y	Composition, mol.%			Phase composition	T_m, °C
		Al_2O_3	ZrO_2	Ln_2O_3		
1.	La	53	27	20	β-Al_2O_3, T, $LaAlO_3$	1665
2.	Ce	53	27	20	β-Al_2O_3, T, $CeAlO_3$	1775*
3.	Pr	53	26	21	β-Al_2O_3, F, $PrAlO_3$	1685
4.	Nd	53	26	21	β-Al_2O_3, F, $NdAlO_3$	1675
5.	Pm	–	–	–	β-Al_2O_3, F, $PmAlO_3$	1785*
6.	Sm	55	25	20	Al_2O_3 + F + $SmAlO_3$	1680
7.	Eu	57	23	20	Al_2O_3 + F + $EuAlO_3$	1580
8.	Gd	60	21	19	Al_2O_3 + F + $GdAlO_3$	1662
9.	Tb	61	21	18	Al_2O_3 + F + $Tb_3Al_5O_{12}$	1745
10.	Dy	62	20	18	Al_2O_3 + F + $Dy_3Al_5O_{12}$	1770
11.	Ho	64	20	16	Al_2O_3 + F + $Ho_3Al_5O_{12}$	1780
12.	Y	65	19	16	Al_2O_3 + F + $Y_3Al_5O_{12}$	1715
13.	Er	65	19	16	Al_2O_3 + F + $Er_3Al_5O_{12}$	1720
14	Tm	65	19	16	Al_2O_3 + F + $Tm_3Al_5O_{12}$	1745
15.	Yb	65	20	15	Al_2O_3 + F + $Yb_3Al_5O_{12}$	1765
16.	Lu	65	20	15	Al_2O_3 + F + $Lu_3Al_5O_{12}$	1840

* Predicted.

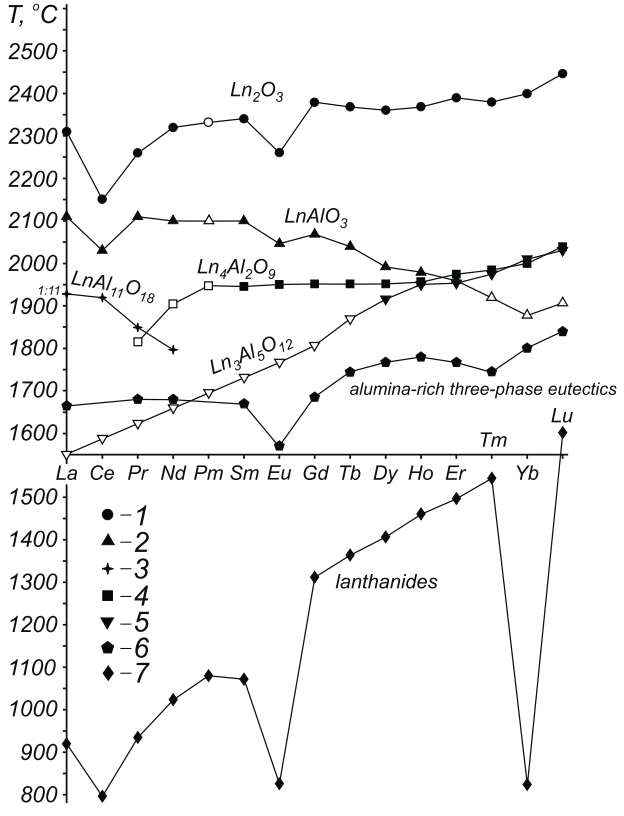

Fig. 7. Experimental and calculated melting temperatures of the compounds in the systems Al_2O_3–Ln_2O_3,[4] lanthanides,[34] their oxides[21] and alumina-rich three-phase eutectics in the Al_2O_3–ZrO_2–Ln_2O_3 systems: 1 – Ln_2O_3; 2 – $LnAlO_3$; 3 – $LnAl_{11}O_{18}$; 4 – $Ln_4Al_2O_9$; 5 – $Ln_3Al_5O_{12}$; 6 – alumina-rich three-phase eutectics; 7 – lanthanides.

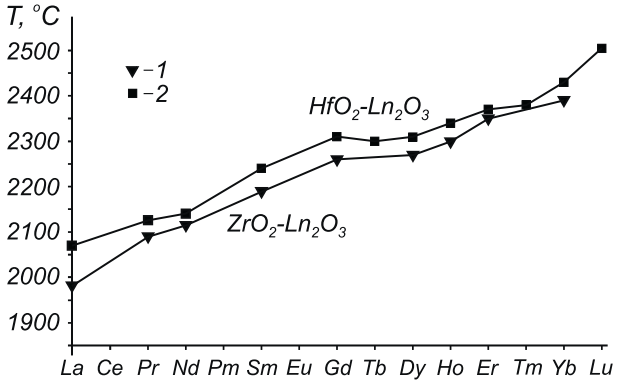

Fig. 8. Dependence of ZrO_2–Ln_2O_3[1,36] and HfO_2–Ln_2O_3[37–40] binary eutectics melting temperatures *vs* lanthanides atomic number: 1 – systems ZrO_2–Ln_2O_3; 2 – systems HfO_2–Ln_2O_3.

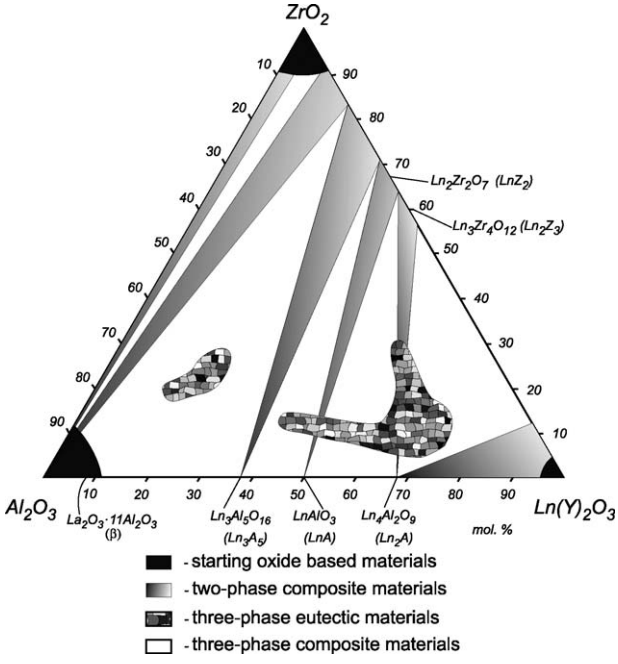

Fig. 9. Concentration areas in the Al_2O_3–ZrO_2–$Ln(Y)_2O_3$ systems in which new materials for different industrial applications are perspective to construct.

directionally solidified eutectics (DSE), etc. are represented. Before constructing phase diagrams of the Al_2O_3–ZrO_2–$Ln(Y)_2O_3$ systems the areas of applications were localized mainly near components. As a result of these investigations wide two- and three-phase areas were discovered, in which numbers of structural, heat-protecting and functional materials can be produced.

4. Conclusions

Phase equilibria in the ternary systems Al_2O_3–ZrO_2–Ln_2O_3 (Ln = La, Nd, Sm, Gd, Er, Yb and Y) were investigated by identical methods in all range of concentrations and 1250–2700 °C temperature range and their phase diagrams were constructed. They revealed that no quasiternary compounds and appreciable regions of solid solutions based on quasibinary compounds and components were found in the systems. Phase transformations $^{F\leftrightarrows T}$ of ZrO_2-based solid solutions and $^{X\leftrightarrows H\leftrightarrows A\leftrightarrows B\leftrightarrows C}$ of Ln_2O_3-based solid solutions realize as liquid involving transformation processes. Thermal stability of compounds-superstructures with the pyrochlore-type structure $Ln_2Zr_2O_7$ and with rhombohedral structure $Zr_3Ln_4O_{12}$ formed in the binaries ZrO_2–Ln_2O_3 does not change with adding third component (Al_2O_3). Solidification in the systems finishes in eutectic equilibria in the areas close to the binary bounding systems Al_2O_3–$Ln(Y)_2O_3$. The established interaction regularities allowed to forecast interaction and phase diagrams construction in systems with other lanthanides (Ce, Pr, Pm, Eu, Tb, Dy, Ho, Tm, Lu). The limited experiments confirmed the forecast. Alumina-rich three-phase eutectics demonstrate cooperative eutectic growth, so they can be obtained as three-phase "in situ" composite by directional solidification.

References

1. Rouanet A. Contribution a l'etude des systemes zircone-oxydes des lanthanides au voisinage de la fusion. *Rev Int Hautes Temper Refract* 1971;**8**:161–80.
2. Bondar IA, Shirvinskaya AK, Popova VF, Mochalov IV, Ivanov AO. Thermal stability of orthoaluminates of rare-earth elements of yttrium subgroup. *DAN SSSR* 1979;**246**:1132–6 [in Russian].
3. Mizuno M. Phase diagrams of the systems Al_2O_3–Ho_2O_3 and Al_2O_3–Er_2O_3 at high temperatures. *J Ceram Soc Jpn* 1979;**87**:405–12.
4. Wu P, Pelton AD. Coupled thermodynamic-phase diagram assessment of the rare earth oxide–aluminium oxide binary systems. *J Alloys Compd* 1992;**179**:259–87.
5. Lakiza SM, Lopato LM. Stable and metastable phase relations in the system alumina–zirconia–yttria. *J Am Ceram Soc* 1997;**80**:893–902.
6. Stubican VS, Hink RC, Ray SP. Phase equilibria and ordering in the system ZrO_2–Y_2O_3. *J Am Ceram Soc* 1978;**61**:17–21.
7. Cocayne B. The uses and enigmas of the Al_2O_3–Y_2O_3 phase system. *J Less-Com Met* 1985;**114**:199–206.
8. Mizuno M, Berjoan R, Coutures JP, Foex M. Phase diagram of the system Al_2O_3–La_2O_3 at elevated temperatures. *J Ceram Soc Jpn* 1974;**82**:631–6.
9. Couture JP. The Al_2O_3–Nd_2O_3 phase diagram. *J Am Ceram Soc* 1985;**68**:105–7.
10. Mizuno M, Yamada T, Noguchi T. Phase diagram of the system Al_2O_3–Sm_2O_3 at high temperatures. *J Ceram Soc Jpn* 1977;**85**:374–9.
11. Mizuno M, Yamada T, Noguchi T. Phase diagram of the systems Al_2O_3–Eu_2O_3 and Al_2O_3–Gd_2O_3 at high temperatures. *J Ceram Soc Jpn* 1977;**85**(11):543–8.
12. Gervais M, Douy A. Solid phase transformation and melting of the compounds $Ln_4Al_2O_9$ (Ln = Gd, Dy, Y). *Mater Sci Eng* 1996;**B38**: 118–21.
13. Mizuno M, Noguchi T. Phase diagram of the system Al_2O_3–Yb_2O_3 at high temperature. *J Ceram Soc Jpn* 1980;**88**:322–7.
14. Stubican VS, Corman GS, Hellman JR, Senft G. Phase relationships in some ZrO_2 systems. In: *Adv. Ceram.: Proc. II Int. Conf. Sci. Technol. Zirconia, Vol. 12, Science and Technology of Zirconia II*. Stuttgart: The American Ceramic Society; 1983. p. 96–106.
15. Lopato LM, Red'ko VP, Gerasimjuk GI, Shevchenko AV. Synthesis of some rare-earths zirconates (hafnates). *Poroshkovaya Met* 1990;(4):73–5 [in Russian].
16. Yokokawa H, Sakai N, Kawada T, Dokiya M. Phase diagram calculations for ZrO_2 based ceramics: thermodynamic regularities in zirconate formation and solubilities of transition metal oxides. In: *Sci. Technol. Zirconia V*. Lancaster, PA: Technomic Publishing Co.; 1993. p. 59–68.
17. Tuohig WD, Tien TY. Subsolidus phase equilibria in the system ZrO_2–Y_2O_3–Al_2O_3. *J Am Ceram Soc* 1980;**63**:595–6.
18. Popov SG, Pashin SF, Paromova MV, Kulikova ZJa, Sch.Rozanova N, Klimenko AN, et al. Subsolidus phase equilibria in the ZrO_2–Y_2O_3–Al_2O_3 system. *Izv AN SSSR, Neorgan Mater* 1990;**26**:113–7 [in Russian].
19. Lopato LM, Shevchenko AV, Kuschevsky AE. Investigation of the high-refractory oxide systems. *Poroshkovaya Metalurgiya* 1972;**1**:88–92 [in Russian].
20. Shevchenko AV, Tkachenko VD, Lopato LM, Ruban AK, Pasdichny VV. Determination procedure of phase transition temperatures by using solar heating. *Poroshkovaya Metalurgiya* 1985;**1**:91–5 [in Russian].
21. Red'ko VP. Physiko-chemical investigation of the compounds $M_4Zr(Hf)_3O_{12}$ in the systems $ZrO_2(HfO_2)$–rare-earths oxides. PhD in chemistry; 1990. p. 152–68 [in Russian].
22. Lakiza S, Fabrichnaya O, Wang Ch, Zinkevich M, Aldinger F. Phase diagram of the ZrO_2–Gd_2O_3–Al_2O_3 system. *J Eur Ceram Soc* 2006;**26**(3):233–46.
23. Lakiza S, Fabrichnaya O, Zinkevich M, Aldinger F. On the phase relations in the ZrO_2–$YO_{1.5}$–$AlO_{1.5}$ system. *J Alloys Compd* 2006;**420**:237–45.
24. Lakiza SM, Lopato LM. Phase diagram of the Al_2O_3–ZrO_2–Nd_2O_3 system. *J Eur Ceram Soc* 2006;**26**(16):3725–32.
25. Lakiza S, Lopato L. Phase diagram of the alumina–zirconia–samaria system. *J Am Ceram Soc* 2006;**89**(11):3516–21.
26. Fabrichnaya O, Lakiza S, Wang Ch, Zinkewich M, Aldinger F. Assessment of thermodynamic functions in the ZrO_2–La_2O_3–Al_2O_3 system. *J Alloys Compd* 2008;**453**:271–81.
27. Lakiza SM, Lopato LM. Phase diagram of the Al_2O_3–ZrO_2–Er_2O_3 system. *J Eur Ceram Soc* 2008;**28**(12):2389–97.
28. Lakiza SM, Zaitseva ZO, Lopato LM. The Al_2O_3–ZrO_2–Yb_2O_3 phase diagram. II. Liquidus surface. *Powder Met Met Ceram* 2008;**47**(5-6): 338–43.
29. Lakiza SM, Red'ko VP, Lopato LM. The Al_2O_3–ZrO_2–Yb_2O_3 phase diagram. III. Solidus surface and phase equilibria in alloys solidification. *Powder Met Met Ceram* 2008;**47**(7-8):420–7.
30. Waku Y, Sakata S, Mitani A, Shimizu K, Hasebe M. Temperature dependence of flexural strength and microstructure of $Al_2O_3/Y_3Al_5O_{12}/ZrO_2$ ternary melt growth composites. *J Mater Sci* 2002;**37**:2975–82.
31. Murayama Y, Hamada S, Lee JH, Yoshikawa A, Shimizu K, Nakagawa N, et al. High-temperature strength of directionally solidified Al_2O_3/YAG/ZrO_2 eutectic composite. *Mater Sci Forum* 2005;**475–479**:1295–300.
32. Waku Y, Sakata S, Mitani A, Shimizu K. High-temperature strength and a microstructure of an $Al_2O_3/Er_3Al_5O_{12}/ZrO_2$ ternary MGC. *J Jpn Inst Met* 2000;**64**:1263–8.
33. Nakagawa N, Ohtsubo H, Waku Y, Yugami H. Thermal emission properties of $Al_2O_3/Er_3Al_5O_{12}$ eutectic ceramics. *J Eur Ceram Soc* 2005;**25**:1285–91.
34. Nekrasov BV. Fundamentals of general chemistry, 3 vol. In: *Chemistry*, vol. 2. Moskov; 1967. 400 p. [in Russian].
35. Samsomov GV, Gilman IJa. Electron structure and physical properties of lanthanides oxides. *Kyiv, Inst Probl Mater Sci, AS USSR* 1975:26 [in Russian].

36. Lopato LM, Andrievskaya ER, Shevchenko AV, Red'ko VP. Phase correlations in the system ZrO_2–Eu_2O_3. *J Inorg Chem* 1997;**42**(10):1736–9 [in Russian].
37. Shevchenko AV, Lopato LM, Zajceva ZA. Interaction of HfO_2 with lanthanum, praseodymium and neodymium oxides at high temperatures. *Izv AN SSSR, Neorgan Mater* 1984;**20**:1530–4 [in Russian].
38. Shevchenko AV, Lopato LM, Nazarenko LV. The systems of HfO_2 with samarium, gadolinium, terbium and dysprosium oxides at high temperatures. *Izv AN SSSR, Neorgan Mater* 1984;**20**: 1862–6.
39. Shevchenko AV, Lopato LM, Kirjakova IE. Interaction of HfO_2 with Y_2O_3, Ho_2O_3, Er_2O_3, Tm_2O_3, Yb_2O_3 and Lu_2O_3 at high temperatures. *Izv AN SSSR, Neorgan Mater* 1984;**20**:1991–4.
40. Andrievskaya ER, Lopato LM, Shevchenko AV, Smirnov VP. Interaction in the system HfO_2–Eu_2O_3. *Izv RAN, Neonorgan Mater* 1997;**33**(7):836–8 [in Russian].